Enhancing Transient Dynamics Stabilization in Islanded Microgrids Through Adaptive and Hierarchical Data-Driven Predictive Droop Control

Apoorva Nandakumar, Yan Li, *Senior Member, IEEE*, Zhe Xu, *Member, IEEE*, and Daning Huang, *Member, IEEE*

***Abstract*—The transient dynamics of microgrids is primarily impacted by low-inertia power electronic interfaces, energy generation of distributed energy resources (DERs), load demand fluctuations, and the control strategies employed for system integration. This paper focuses on the enhancement of the transient dynamics to achieve a stable steady-state operation for the microgrid by minimizing the overall islanded system's frequency deviations. A modularized physics-informed sparse identification technique is developed for system identification that can accurately predict the future states of the microgrid with interconnected DERs. The data-driven prediction model is then incorporated into the model predictive control framework to generate an optimal control input that can augment with conventional droop control for frequency stabilization. Given the inherent fluctuations in typical microgrid operations, stemming from factors such as varying load demands, weather conditions, and other variables, reachability analysis is also performed in this work. By doing so, we aim to facilitate the design of data-driven models and implement effective control strategies for microgrids subject to disturbances, and thus, ensuring the safety, reliability, and efficiency of microgrids across a wide range of operating conditions. The effectiveness of the proposed approaches is verified in this paper with numerical examples where the developed controller is tested in various worst-case scenarios generated by the reachable set computation.**

***Index Terms*—Microgrids, physics-informed data-driven modeling, sparse identification, model predictive control, reachability, droop control.**

I. Introduction

A MICROGRID is a cluster of micro-sources, storage systems and loads which presents itself to the grid as a single entity that can respond to central control signals [1], [2].

Manuscript received 4 August 2023; revised 23 December 2023 and 27 May 2024; accepted 9 August 2024. Date of publication 4 September 2024; date of current version 26 December 2024. This work was supported in part by the National Science Foundation under Award DMS-2229435, and in part by the Office of Naval Research under Award N00014-22-1-2504. Paper no. TSG-01218-2023. *(Corresponding author: Yan Li.)*

Apoorva Nandakumar and Yan Li are with the Department of Electrical Engineering, The Pennsylvania State University, University Park, PA 16802 USA (e-mail: yql5925@psu.edu).

Zhe Xu is with the Department of Aerospace and Mechanical Engineering, School for Engineering of Matter, Transport and Energy, Arizona State University, Tempe, AZ 85281 USA.

Daning Huang is with the Department of Aerospace Engineering, The Pennsylvania State University, University Park, PA 16802 USA.

Color versions of one or more figures in this article are available at https://doi.org/10.1109/TSG.2024.3448460.

Digital Object Identifier 10.1109/TSG.2024.3448460

Microgrids are increasingly being considered as a cost-effective option for power supply in remote or off-grid areas. They offer greater access to electricity supply that is highly reliable and resilient [3]. Microgrids can operate in islanded mode, connected to the distribution network, or connected to other microgrids [4]. An islanded microgrid refers to a standalone power system that is disconnected from the main grid and operates independently. Microgrid control involves managing and optimizing the distributed energy resources (DERs) in the different operating modes to ensure a stable, reliable, and efficient energy supply [2], [5]. Traditional frequency and voltage droop control strategies without using vector control techniques were used to share real and reactive powers among two or more DER units. However, this would cause a significant challenge in reactive power sharing among DGs, a low power quality, issues associated with voltage instability, and great difficulty to reconnect MGs and DERs to grid-tied mode [6], [7].

Microgrid control can also be classified based on the location of the controllers with respect to the inverters as centralized and de-centralized controls [8], [9]. In centralized control schemes, there is one control scheme/unit that is used to govern all inverters; it's more convenient for smaller microgrids. If each of inverter has its own control scheme in the decentralized control scheme, this scheme becomes more suitable for medium-size and large-size microgrids [10], [11], [12]. A robust droop control algorithm is discussed in [13]. While it has multiple advantages in controlling the microgrid to operate in a stable manner under extreme non-linearities and uncertainties, the method can have a slow response time.

Model Predictive Control (MPC) is a control strategy that uses a model of the system to predict future behavior and determine optimal control inputs. MPC offers several advantages over other traditional microgrid control strategies, including improved efficiency, flexibility, stability, integration of renewable energy, and scalability. It can help microgrid operators to optimize their energy management, reduce operating costs, and improve overall system performance. It can be cascaded with the previously discussed methods to provide additional control to the system to enable increased stability and improved flexibility [14], [15].

Model development for prediction is extremely crucial in MPC as it helps to anticipate the future behavior, enabling

informed decision-making and optimization in various applications. However, uncertainties in the model parameters, disturbances, and unmodeled dynamics can lead to prediction errors. Model uncertainties can degrade the overall control performance. One of the most common approaches to overcome the challenges involved in model development is to utilize data-driven methods such as machine learning or data mining techniques to develop models. These approaches can leverage large data sets and uncover hidden patterns or relationships in the data, resulting in more accurate predictions [16], [17], [18], [19], [20]. While it is advantageous to model complex systems whose mechanisms are not well understood, data-driven models may not be able to capture the underlying physics accurately without abundance of data [21].

A physics-informed data-driven model incorporates prior knowledge and assumptions about the underlying physics or mechanisms into the model construction process and uses data to further refine and validate the model. This approach aims to improve the accuracy and physical consistency of the model by leveraging the strengths of both the approaches. The purpose of developing mixed approaches is to improve the reliability of the obtained relations through fundamental principles [22], [23]. A physics-informed neural network with sparse regression has been discussed in [24] which possesses the salient features of interpretability and generalizability, to discover governing PDEs of nonlinear spatiotemporal systems from scarce and noisy data. Another advantage of physics informed data-driven modeling is its flexibility and adaptability. It can be easily updated and retrained with new data, allowing them to adapt to changing conditions and environments. They can also be easily integrated with other models or systems, such as control systems or optimization algorithms [25]. Developing a reliable data-driven model involves the use of statistical and machine learning techniques in combination with a physics based approach to extract patterns and relationships that can be used to make future predictions. These models are often based on simple and interpretable functions, such as linear or nonlinear regression models, decision trees, or neural networks [26].

In the context of microgrid dynamics, MPC can be used to optimize the operation of DERs, such as renewable energy sources, energy storage systems, and controllable loads. The MPC algorithm computes a control sequence that minimizes a cost function, such as the operating cost or the carbon emissions, subject to constraints on the system variables, such as the power balance and the state of charge of the energy storage systems. MPC can ensure that the DERs operate within their physical limits and that the power balance is maintained, even in the presence of stochastic variations in the renewable energy sources [27] and the load demand. To implement MPC in microgrids, a dynamic model of the system is required. This model can be derived from first principles or can be identified from data using system identification techniques. Two major challenges in implementing the MPC are listed below:

1. It is difficult to obtain an accurate prediction model which has an interpretable closed-form expression and is consistent with the basic physical laws.
2. The microgrid system features are not deterministic and the developed model should have the capability to address the uncertainties in the system.

Reachability analysis is a technique for analyzing the behavior of a system by computing its reachable set, which is the set of all states that can be reached from a given initial state, subject to constraints on the system dynamics and control inputs. It can be defined as computing the set of states that are reachable by a dynamical system from all initial states and for all admissible inputs and parameters. It is a fundamental problem motivated by many applications in formal verification, controller synthesis, and estimation, to name only a few [28].

In the context of microgrids, reachability analysis can be used to evaluate the performance and safety of the system under different operating conditions [29]. By computing the reachable set and identifying the set of possible system models, reachability analysis can help in designing data-driven models and control strategies for microgrids that are safe, reliable, and efficient.

MPC and reachability analysis can be used in conjunction to incorporate the reachable set into the MPC optimization problem [30], [31], [32]. This can be done by adding constraints on the reachable set to the MPC problem, which can improve the robustness and safety of the control strategy. For example, by constraining the MPC solution to lie within the reachable set, the controller can ensure that the system will not violate safety constraints even in the presence of uncertainties or disturbances. Another way to use MPC and reachability analysis together is to use reachability analysis to compute the least optimistic system model for MPC. This can be done by using reachability analysis to identify the set of possible system models that are consistent with the available data and using these models in the MPC optimization problem. This can improve the accuracy and robustness of the control strategy, as it can capture the uncertainties and nonlinearities in the system dynamics more effectively. This work employs reachability analysis to determine the efficiency of the proposed MPC to control the transients in the least optimistic cases.

The major contributions of this paper are summarized as follows:

1. A hierarchical multi-layered modularized sparse identification algorithm is developed in this paper to capture the non-linearities in the microgrid transient dynamics. This method is successful in predicting the future operating states of the microgrid model under various disturbances since the primary layer of the developed algorithm is built using the prior knowledge of the various non-linearities that are typically present in the power systems domain. This method of identification has a lower reliance on the data and is computationally efficient. The modularization aspect of the proposed identification algorithm can be used for extending the model to predict the dynamics of a scaled and reconfigured system.
2. The islanded microgrid is sensitive to disturbances and the traditional droop controller has a slow transient response, taking a significant amount of time to stabilize the system. The prediction horizon of the model

predictive controller (MPC) is developed based on a novel hierarchical multi-layer sparse regression based prediction model and is cascaded along with the traditional droop controller to develop an adaptive droop control that can quickly stabilize the frequency of the overall system.

3. The advantages of adaptive control is combined with that of model predictive control in this work. While the MPC can handle the input disturbances through its optimization process, adaptive control addresses the unmodeled disturbances that might not be explicitly considered in the standalone MPC model. In this paper, an algorithm is designed to quickly stabilize the transient dynamics in the microgrid system and reach the desired steady state operation.
4. The microgrid dynamics are more stochastic in nature due to the inherent variability of renewable energy sources which are subject to fluctuations in input such as external weather conditions and topology changes. It is important to understand the possible operating region of the microgrid system under various conditions to develop the model predictive control algorithm so that the system is robust to multiple input variations and initial conditions. Reachability analysis is leveraged and developed as a powerful tool to determine the variable operations of the microgrid and quantify the performance of the developed controller.
5. A robust model predictive controller explicitly accounts for uncertainties in the system and attempts to optimize the controller performance in the worst-case scenarios within the uncertainty set. The set-based methods are used to compute the reachable set of the system which accounts for uncertainties in the system parameters.

The remainder of the paper is organized as follows. Section II outlines the overall idea of the transient dynamics stabilization by the development of an adaptive droop controller which stems from the conjunction of MPC and traditional droop controller. The predictive model development using a physics informed data driven technique is also discussed in detail. Finally, the section describes the need for the reachable set computation and the impact of the combination og MPC and reachable set. Section III provides numerical examples to verify and validate the efficiency of the proposed algorithm. Conclusions are drawn in Section IV.

II. Theoretical Contributions

A. Modeling of Microgrid Transient Dynamics

Modeling of the transient dynamics in a microgrid involves capturing the system's dynamic response to disturbances or changes in the operating conditions. The overall transient dynamics model of a microgrid integrates the individual dynamic models of generators, energy storage elements, power electronics, and loads to capture their interactions and their system response accurately. Mathematically, this integration can be achieved by modeling the microgrid system as a set of nonlinear differential algebraic equations (DAEs) [33], [34] when the power-electronic interfaces are modeled using dynamic averaging. This is given by Eq. (1).

$$\dot{\mathbf{x}}(t) = \mathbf{f}(\mathbf{x}(t), \mathbf{y}(t), \mathbf{u}(t)), \tag{1a}$$

$$\mathbf{0} = \mathbf{g}(\mathbf{x}(t), \mathbf{y}(t), \mathbf{u}(t)), \tag{1b}$$

where $\mathbf{x} \in \mathbb{R}^n$ is the state variable vector, e.g., state variables in the controller of DER power-electronic interfaces, $\mathbf{y} \in \mathbb{R}^m$ is the algebraic variable vector, e.g., bus voltage amplitude and angle, line currents, and $\mathbf{u} \in \mathbb{R}^p$ represents the input variations/ disturbances, e.g., power output fluctuation of the DERs and power load changes.

B. System Identification and Prediction

Sparse Identification of Nonlinear Dynamics (SINDy) is a data-driven method that is used for the discovery of governing equations of dynamical systems from observational data [35], [36], [37]. Modularized sparse identification method realizes distributed discovery of nonlinear dynamics by partitioning a higher-order microgrid system into multiple subsystems and introducing pseudo-states to represent the impact of neighboring subsystems [38].

1) Preliminaries on Modularized SINDy With Control for Modeling the Microgrid Transient Dynamics: The time series data required for the system identification includes the state variables ($\mathbf{x}(t)$), the algebraic variables ($\mathbf{v}(t)$ and $\mathbf{i}(t)$) and the input disturbance variables ($\mathbf{u}(t)$). After identifying the variables corresponding to the different modules in the system ($\mathbf{x}_j$ represents the states corresponding to the j^{th} module) based on the microgrid generational units as shown in Eq. (2) and Eq. (3), the data set is denoted.

$$\mathbf{X_j} = \begin{bmatrix} \mathbf{x_j}^\mathsf{T}(t_1) & \mathbf{x_j}^\mathsf{T}(t_2) & \cdots & \mathbf{x_j}^\mathsf{T}(t_k) \\ \mathbf{v_j}^\mathsf{T}(t_1) & \mathbf{v_j}^\mathsf{T}(t_2) & \cdots & \mathbf{v_j}^\mathsf{T}(t_k) \\ \mathbf{i_j}^\mathsf{T}(t_1) & \mathbf{i_j}^\mathsf{T}(t_2) & \cdots & \mathbf{i_j}^\mathsf{T}(t_k) \end{bmatrix}^\mathsf{T} \tag{2}$$

$$\mathbf{U_j} = \begin{bmatrix} \mathbf{u_j}^\mathsf{T}(t_1) & \mathbf{u_j}^\mathsf{T}(t_2) & \cdots & \mathbf{u_j}^\mathsf{T}(t_k) \end{bmatrix}^\mathsf{T} \tag{3}$$

A simple set of candidate functions is represented by Eq. (4). Here, $\mathbf{X}_j^{P2}$ represents the second order polynomial terms of $\mathbf{X}_j$. Similarly, $\sin(\mathbf{X}_j)$ and $\cos(\mathbf{X}_j)$ represents the sinusoidal terms of $\mathbf{X}_j$.

$$\begin{aligned} \Theta(\mathbf{X_j}, \mathbf{U_j}) = \Big[& \mathbf{1} \quad \mathbf{X_j} \quad \mathbf{X_j}^{P^2} \quad \cdots \\ & \sin(\mathbf{X_j}) \quad \cos(\mathbf{X_j}) \quad \mathbf{U_j} \quad \mathbf{X_j U_j} \quad \cdots \\ & \sin(\mathbf{U_j}) \quad \cos(\mathbf{U_j}) \quad \cdots \quad \mathbf{X_j} \sin(\mathbf{X_j}) \quad \cdots \Big] \end{aligned} \tag{4}$$

The final step of system identification is the sparse regression of the data set to identify the governing equations of the modules. The transient dynamics of the microgrid can be modeled using only a few terms from the set of all non-linear candidate functions. Thus, the linear combination of non-linear terms that would accurately describe the system's governing equations can be obtained using the sparse regression method. If the sparse vector coefficients identified using regression

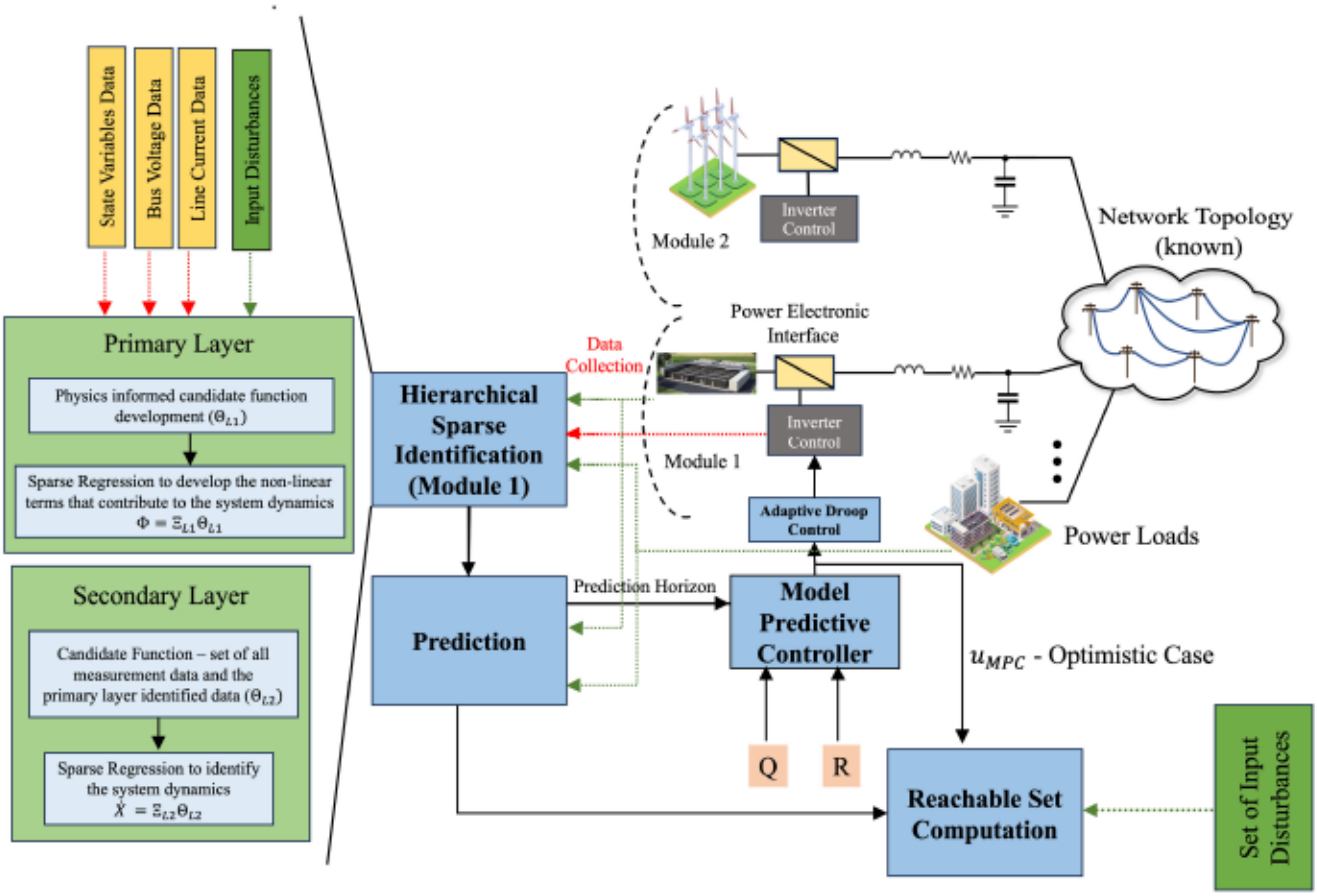

Fig. 1. Schematic representation of the overall algorithm.

is given by $\Xi = [\xi_1 \quad \xi_2 \quad \cdots \quad \xi_s]$, then $\dot{\mathbf{X}}$ can be represented as,

$$\dot{\mathbf{X}}_j = \Xi\Theta^{\mathsf{T}}(\mathbf{X_j}, \mathbf{U_j}), \tag{5}$$

2) Physics-Informed Hierarchical Sparse Identification for Prediction: While the basic SINDy algorithm can be used for the overall model identification, this paper focuses on the development of a physics-informed modular sparse identification technique because:

1. The incorporation of physical principles to the data driven technique acts as a regularization mechanism. It constrains the model to conform to the physical laws and can avoid fitting irrelevant features in the data and provide more reliable predictions.
2. A physics-informed data-driven model can achieve more accurate predictions with lesser training data. This method requires fewer training samples to learn the underlying dynamics accurately which is particularly valuable while collecting large amounts of training data as the data collection process can be expensive and time-consuming.

In the context of microgrid modeling, the terms that contribute to the system non-linearities arises from the trigonometric and quadratic non-linearities.

The trigonometric non-linearity stems from the dq transformation that is used to convert a three-phase signal into two orthogonal components, namely the d-axis and the q-axis. This simplifies the analysis and control of the three-phase systems. The d-axis component is proportional to the average value of the three-phase signal, while the q-axis component is proportional to the quadrature component of the three-phase signal.

The dq transformation is a mathematical tool used in power systems to convert a set of voltage or current phasors in a rotating reference frame into a two-dimensional space in the dq reference frame.

$$\begin{bmatrix} V_d \\ V_q \end{bmatrix} = \begin{bmatrix} \cos(\theta) & \sin(\theta) \\ -\sin(\theta) & \cos(\theta) \end{bmatrix} \begin{bmatrix} V_{\mathrm{R}} \\ V_{\mathrm{I}} \end{bmatrix} \tag{6}$$

$$\begin{bmatrix} I_d \\ I_q \end{bmatrix} = \begin{bmatrix} \cos(\theta) & \sin(\theta) \\ -\sin(\theta) & \cos(\theta) \end{bmatrix} \begin{bmatrix} I_{\mathrm{R}} \\ I_{\mathrm{I}} \end{bmatrix} \tag{7}$$

The dq transformation was developed to simplify the control of the power electronic converters, as it separates the control of the active and reactive power flows [39]. Additionally, this property is leveraged in this paper to develop the modulars based on d-axis state variables and q-axis state variables to improve the efficiency of the physics informed sparse identification.

The voltage magnitude is another important parameter that is used to describe the state of the system. The non-linearity of this term arises from the following quadratic equation

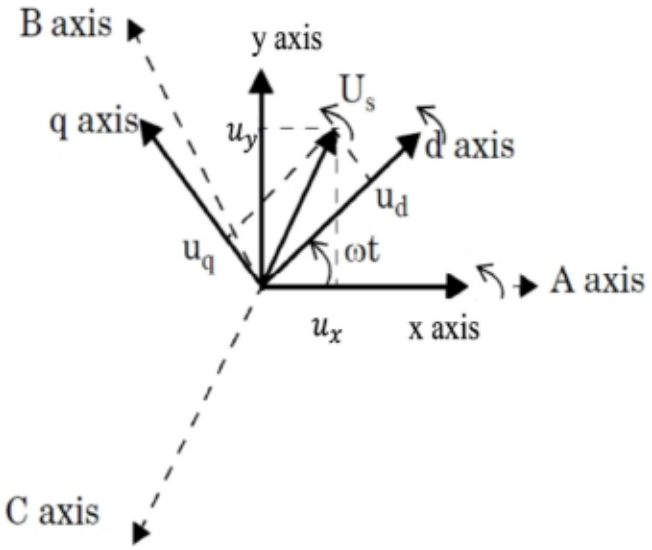

Fig. 2. Reference frame for voltage and line current phasor transformation.

formulation:

$$V_m = \sqrt{V_\alpha^2 + V_\beta^2} \tag{8}$$

Based on the prior knowledge of the non-linear terms in the set of the DAEs that describe the microgrid transient dynamics, a hierarchical modular sparse identification method is introduced in this paper to simplify the process of system identification with an improved computational efficiency.

The input data required for the primary layer of the hierarchical sparse identification model consists of the system state variables ($\mathbf{x}(t)$), output bus voltage (real and imaginary components) ($\mathbf{v}(t)$) and line current data (real and imaginary components) ($\mathbf{i}(t)$). This is given by Eq. (9), which is a rearrangement of Eq. (2).

$$\mathbf{X_{L1}} = \begin{bmatrix} x_1(t_1)\cdots x_n(t_1) & v_1(t_1)\cdots v_p(t_1) & i_1(t_1)\cdots i_p(t_1) \\ x_1(t_2)\cdots x_n(t_2) & v_1(t_2)\cdots v_p(t_2) & i_1(t_2)\cdots i_p(t_2) \\ \vdots & \vdots & \vdots \\ x_1(t_m)\cdots x_n(t_m) & v_1(t_m)\cdots v_p(t_m) & i_1(t_m)\cdots i_p(t_m) \end{bmatrix} \tag{9}$$

The library of candidate functions for the first layer of the hierarchical SINDy can be established as:

$$\Theta_{L1}(\mathbf{X},\mathbf{V},\mathbf{I}) = \begin{bmatrix} \mathbf{1} & \mathbf{X} & \mathbf{X}^{P2} & \cdots & & \sin(\mathbf{X}) \\ \cos(\mathbf{X}) & \mathbf{V} & \mathbf{XV} & \cdots & \sin(\mathbf{V}) & \cos(\mathbf{V}) \\ \cdots & \mathbf{I} & \mathbf{XI} & \cdots & \sin(\mathbf{I}) & \cos(\mathbf{I}) \\ \cdots & \mathbf{X}\sin(\mathbf{X}) & \cdots & \mathbf{I}\sin(\mathbf{X}) & \mathbf{V}\sin(\mathbf{X}) & \cdots \end{bmatrix} \tag{10}$$

Sparse Regression is performed to identify these special non-linear terms ($\mathbf{\Phi}(t)$) using input data sent to the first layer using the basic sparse regression algorithm discussed in the previous subsection. The output of the primary layer consists of the voltage magnitude, and the bus voltages and line currents in the d-q framework.

In addition to the already gathered system state variables data, the identified non-linear functional data, represented by $\mathbf{\Phi}(t)$ are added to develop the input data for the second layer of the hierarchical modularized SINDy model. The entire microgrid is decomposed into multiple subsystems, each subsystem consisting of the variables belonging to the individual generators.

Algorithm 1: Sparse Regression of Nonlinear Dynamics

Data:
Input Data:
System State Variables, Input Disturbances, Primary Layer Output (Inverter dq-axis Voltage, Inverter dq-axis Line Current)
Features:
System Transient Dynamics based on $\mathbf{f}(x, y, u)$
Result:
Identified Ξ matrix based on LASSO regression

Step 1: Set Regularization Parameter $\lambda = 0.1$
Step 2: **while** $i \leftarrow 1 : 100$ **do**
  Update the intercept term - coefficient matrix Ξ
  Check for convergence to verify if change of coefficients is below a given threshold
  $\Xi = \arg\min_{\Xi'} ||\mathbf{\Theta}\Xi' - \mathbf{X}||_2 + \lambda||\Xi'||_1$
end while

$$\Theta_{L2}^{g1}\left(\mathbf{X}^{g1}, \mathbf{\Phi}^{g1}, \mathbf{U}^{g1}\right) = [1 \quad \mathbf{X}^{g1} \quad \mathbf{\Phi}^{g1} \quad \mathbf{U}^{g1}] \tag{11}$$

Furthermore, the states, voltages and non-linearities within each generator are split into d-axis and q-axis components to simplify the overall identification.

Here, $\mathbf{X}$ is the set of all the state variables. $\mathbf{\Phi}$ is the output of the first layer of the developed model which comprises of the algebraic terms contributing to the non-linearity in the model. $\mathbf{U}$ is the external disturbances that drives the system dynamics.

$$\dot{\mathbf{X}}^{g1} = \Xi_{L2}^{g1}\Theta_{L2}^{g1\mathsf{T}}\left(\mathbf{X}^{g1}, \mathbf{\Phi}^{g1}, \mathbf{U}^{g1}\right) \tag{12}$$

Ξ_{L2}^{g1} is the sparse vector coefficients identified by regression for the first generator. The set of all the sparse vector co-efficients can be put together to identify the overall microgrid system.

$$\Xi = \left[\Xi_{L2}^{g1} \quad \Xi_{L2}^{g2} \quad \cdots \quad \Xi_{L2}^{gn}\right] \tag{13}$$

The algebraic part of the microgrid model represents the network topology and these details are assumed to be known to the system operator.

The sparse regression algorithm to learn and tune the coefficients Ξ matrix of primary and secondary layer to fit the terms of $\mathbf{\Theta}_{L1}$ and $\mathbf{\Theta}_{L2}$ to determine the microgrid's transient dynamics $\mathbf{f}(x, y, u)$ is given by Alg. 1.

The identified Ξ matrix can be used to develop the prediction model. Based on the predictive model, a model predictive controller with quadratic loss can be used to stabilize the frequency deviations more quickly in the microgrid system, as discussed in the following sections.

C. Adaptive Droop Controller for Microgrids

Droop control is a widely used technique in microgrids to achieve decentralized power sharing and voltage regulation among DERs. In a droop-controlled microgrid, each DER adjusts its output based on the deviation from the nominal frequency or voltage, allowing for a decentralized and self-regulating operation [40].

In a droop-controlled system, when the system parameter deviates from its nominal value (such as frequency or voltage), each generator adjusts its output power (or voltage) based on its droop characteristic. This adjustment helps maintain power balance, share the load, and regulate system parameters within acceptable limits. The typical $P-\omega$ and $Q-V$ droop characteristics are described in [40]. The mathematical equation to describe conventional droop characteristic of a single generator is illustrated by Eq. (14) and Eq. (15).

$$f = f^* - K_P(P^* - P) \tag{14}$$
$$V = V^* - K_Q(Q^* - Q) \tag{15}$$

Here, f, V, P, Q are the frequency, voltage, active power output and reactive power output of the generator. K_P and K_Q represents the frequency droop coefficient and the voltage droop coefficient. f^*, V^*, P^*, Q^* are the initial nominal values. The inherent trade-off in a conventional droop controller lies in the selection of the droop coefficient value. Increasing the droop coefficients results in good power sharing but a degraded voltage regulation [41]. The conventional droop technique also has a slow transient response and poor steady state performance with multiple renewable energy resources. A modified droop controller has been proposed in this paper with adaptive droop coefficients to improve the transient stability of the system by utilizing the concept of model predictive control.

The proposed adaptive droop controller is effective in minimizing the transients in the overall system frequency. In an islanded microgrid, frequency is controlled by the power balance between generation and load within the microgrid and is sensitive to the power imbalances caused by the variations in load demand or fluctuations in generation output. The equations of the voltage and frequency of the microgrid developed based on the adaptive droop controller are shown in Eq. (16) and Eq. (17). Here, u_m and u_n are the control inputs generated by MPC to convert the traditional droop controller into adaptive droop controller. The frequency deviation ($\Delta\omega$) is responsible for the transients in one of the state variables of $\mathbf{f}(\cdot)$ and is determined based on the droop slope between frequency and active power generation. This term is also used to add the dynamics constraint to the model predictive controller. In a typical microgrid system, the droop coefficients are fixed in the controller. The proposed adaptive droop controller actively updates the droop coefficients to determine the frequency reference $\bar{\Delta\omega}$ for the DER.

$$f = f^* - K_P(P^* - P)u_m \tag{16}$$
$$V = V^* - K_Q(Q^* - Q)u_n \tag{17}$$

D. Parameter Design for Adaptive Droop Controller Using Model Predictive Control

Model Predictive Control takes full advantage of the developed system model under specific constraints to gain better control signals by minimizing predefined cost functions [42]. Constraints on the state and output variables of interest are usually formulated inside the cost function. The general format of cost function considering the Euclidean distance between the predicted and the desired values is usually expressed as:

$$\text{cost} = \Sigma_j\left(W_j|x^* - \tilde{x}(k+1)|\right) \tag{18}$$

Here, x^* is the desired value, W_j is the weight coefficient and $\tilde{x}(k+1)$ is the predicted value. In this paper, the prediction model is developed using the hierarchical modularized physics-informed sparse identification. Typically, the optimal control action of the MPC is developed by observing the system over a finite time horizon. The prediction horizon provides information about the future system behavior and allows the controller to make better decisions.

The physics-informed SINDy-based identification model can be used to determine the N-step predicted states at t_k as $\mathbf{x}(k+1) \rightarrow \mathbf{x}(k+N)$.

The microgrid chosen for this study operates in the islanded mode. Under the different power generations/ load variations and the absence frequency support from the main grid, the primary control objective of the islanded system is to provide a stable frequency/voltage supply. The existence of multiple droop-controlled DERs in the system, requires the generators to adjust their output power to maintain a common frequency across all DERs within a specified range. As discussed in the previous subsection, this causes a slow transient response and a longer time to achieve frequency stabilization.

The objective function is developed to minimize the frequency oscillations across the predicted horizon and reach steady state operation as quickly as possible. For example, if there are two droop controlled DERs in the system (f_1 and f_2 are the corresponding frequencies), the objective is to develop an adaptive droop coefficient, so that $\Delta\omega = 2\pi|f_2 - f_1| \approx 0$. The cost function for this simple case can be developed as:

$$\min_{\Delta\omega_i} \sum_{i=1}^{N} \Delta\omega_i^T Q_{mpc}\Delta\omega_i + u_{m_i}^T R_{mpc} u_{m_i}$$
s.t.
$$\underline{\Delta\omega} \le \Delta\omega_1, \Delta\omega_2, \ldots, \Delta\omega_N \le \overline{\Delta\omega}$$
$$\underline{P} \le P_1, P_2, \ldots, P_N \le \overline{P} \tag{19}$$

$\bar{\Delta\omega}$ defines the reference frequency deviation in the q-axis current controller and $\Delta\omega$ defines the measured frequency deviation. The constraints to calculate the adaptive droop coefficient ($u_m * K_P$) are based on the frequency deviation parameter and the available active power generation. The dynamics of the microgrid can be controlled within the operable limits based on these constraints.

The weights Q_{mpc} and R_{mpc} are chosen to minimize the frequency error and obtain the optimal controls while satisfying the conditions on the bounded constraints. The $\mathcal{L}_2$

Algorithm 2: Algorithm to Compute the Adaptive Model Predictive Droop Controller

Data:
System dynamics function - $\mathbf{f}(\cdot)$, $\mathbf{g}(\cdot)$
Initial adaptive droop parameters - $u_{m_i} = 1$
Initial MPC parameters (based on prediction horizon) -

$$Q_i = \begin{bmatrix} 10 & 0 & \cdots & 0 \\ \vdots & \vdots & \ddots & \vdots \\ 0 & \cdots & 10 & 0 \\ 0 & \cdots & 0 & 10 \end{bmatrix}, R_i = \begin{bmatrix} 10 & \cdots & 0.1 \\ \vdots & \ddots & \vdots \\ 10 & \cdots & 0.1 \end{bmatrix}$$

Result:
Compute u_{m_i} for reduced frequency transients in the microgrid dynamics based on the adaptive model predictive droop controller

while $i \leftarrow t_1 : t_n$ **do**
  Measure the state/ output variables for i^{th} iteration
  while $j \leftarrow t_i : t_{i+p}$ **do**
    Step 1: Compute the system states for the prediction horizon
    Step 2: The goal of the optimization problem is to minimize the cost function

$$\min_{\Delta\omega_i} \sum_{i=1}^{N} \Delta\omega_i^T Q_{mpc} \Delta\omega_i + u_{m_i}^T R_{mpc} u_{m_i}$$

s.t.

$$\underline{\Delta\omega} \leq \Delta\omega_1, \Delta\omega_2, \cdots \Delta\omega_N \leq \overline{\Delta\omega}$$
$$\underline{P} \leq P_1, P_2, \cdots P_N \leq \overline{P} \quad (21)$$

    Step 3: Determine the optimal control signal u_{m_i} determined by the optimization problem
  end while
  Step 4: Implement the control signal to modify the adaptive droop coefficient in the actual system for the next time step
end while

norm is a popular choice for the cost function in MPC because it is easy to compute and has desirable mathematical properties. The $\mathcal{L}_2$ norm is also sensitive to both the magnitude and the direction of the deviation between the predicted and desired outputs, which can make it more informative than other performance metrics. The optimal control solution obtained will be applied to the actual model at $t = t_{k+1}$ to minimize the system transients. Based on the optimal control u_m, the droop equations can be modified as shown in Eq. (20) which incorporates the adaptive droop coefficient to the system and achieves a faster steady state response.

$$f = f^* - K_{P_{\text{mod}}}(P^* - P), K_{P_{\text{mod}}} = K_P u_m \quad (20)$$

To study the robustness of the new adaptive control under different conditions, a reachable set of dynamic responses is developed in the next subsection and the optimistic control u_m is applied to the reachable worst case scenarios.

The algorithm (Algorithm 2.) to represent the model prediction based droop controller formulation is given below.

E. Reachability Analysis

The reachability analysis can bound all the possible trajectories of a dynamic system. It is a set-based approach and incorporates the benefit of time/ frequency domain simulations [43]. The set of intervals on $\mathbb{R}$ is denoted by $\mathbb{IR} = \{\mathcal{A} = [\underline{\mathcal{A}}, \overline{\mathcal{A}}] | \underline{\mathcal{A}}, \overline{\mathcal{A}} \in \mathbb{R}, \underline{\mathcal{A}} \leq \overline{\mathcal{A}}\}$.

Given $f : \mathcal{X} \longrightarrow \mathcal{Y}$ with $\mathcal{X} \subseteq \mathbb{R}^n$ and $\mathcal{Y} \subseteq \mathbb{R}^m$, we define an interval extension of f as an interval valued function $f : \mathbb{IR}^n \longrightarrow \mathbb{IR}^m$ such that

$$f(\mathcal{A}) \supseteq \mathcal{R}(f, \mathcal{A}) = \{f(x) | x \in \mathcal{A}, \vee \mathcal{A} \subseteq \mathcal{X}\} \quad (21)$$

Given a set $\mathcal{I}_i \subseteq \mathcal{X}$ of states at time t_i and a set $\mathcal{V} \subseteq \mathcal{U}$ of control signals, the reachable set of the dynamics at time $t \geq t_i$ is given by $\mathcal{R}(t, \mathcal{I}_i, \mathcal{V}) = \{z \in \mathcal{X} | \exists x_i \in \mathcal{I}_i, \exists v \in \mathcal{V}, z = x(t, x_i, v)\}$ [44].

The external input disturbances contributing to the microgrid transient dynamics can be the non-linear load changes or the active and reactive power generations at the different DERs. In order to quantify the set of possible outcomes caused by these input changes at the different load points and power generations at the non-dispatchable DERs such as the wind or PV, reachability analysis is performed. It is used to study the dynamic behavior of the microgrid system to determine the set of states that the system can reach from the possible set of given initial states and input disturbances.

This paper focuses on the development of a reachable set based analysis to test the reliability of the application of the optimistic control inputs generated by the MPC for the pessimistic cases. Here, $[\mathbf{x}(0), \mathbf{y}(0)] \in \mathcal{R}(0)$ and $u(t) \in \mathcal{U}$. $\mathcal{R}(0)$ is the over-approximated set of the initial states of the microgrid system and $\mathcal{U}$ is the set of possible inputs [45]. We represent a set of input interval on $\mathbb{R}$ as $\mathbb{IR} = \{\mathcal{U} = [\underline{\mathcal{U}}, \overline{\mathcal{U}}], \underline{\mathcal{U}}, \overline{\mathcal{U}} \in \mathbb{R}, \underline{\mathcal{U}} \leq \overline{\mathcal{U}}\}$.

We assume Eq. (1) has a unique solution [46] denoted by $\gamma(t, \mathbf{x}(0), \mathbf{y}(0), \mathbf{u}(\cdot))$ for all the initial states $\mathbf{x}(0) \in \mathbb{R}^{nd}$ and $\mathbf{y}(0) \in \mathbb{R}^{na}$. Here, $\mathbf{u}(\cdot)$ refers to a piecewise continuous input trajectory instead of a single input at a specific point of time. The analysis idea is to find a set of reachable states over some time horizon $t \in [0, t_f]$ as:

$$\mathcal{R}^e([0, t_f]) = \{\gamma(t, \mathbf{x}(0), \mathbf{y}(0), \mathbf{u}(\cdot))| \\ [\mathbf{x}(0), \mathbf{y}(0)] \in \mathcal{R}(0), u(t) \in \mathcal{U}, t \in [0, t_f] \quad (22)$$

The reachable set is the set of all states that can be reached by the system under perfect knowledge of the initial conditions, dynamics, and inputs. The reachable set can be computed using various techniques, such as numerical simulations or analytical methods. However, in practice, it is often impossible to obtain perfect knowledge of these factors, and there may be uncertainties or disturbances in the system that affect its behavior. Therefore, it is often necessary to work with an over-approximation of the reachable set, which is a larger set that includes all possible states that the system could reach, even under worst-case scenarios or in the presence of uncertainties. Thus, we compute $\mathcal{R}([0, t_f]) \supseteq \mathcal{R}^e([0, t_f])$.

Algorithm 3: Algorithm to Compute the Reachable Set

Data:
Initial dynamics states - $x(t_0)$, $y(t_0)$
Initial input set - $u(t_0) \in \mathcal{U}$
System dynamics function - $\mathbf{f}(\cdot)$, $\mathbf{g}(\cdot)$
Result:
Set of all reachable states, $\mathcal{R}([t_0, t_f])$ computed by parsing $\mathcal{U}$ through $\mathbf{f}(\cdot)$ and $\mathbf{g}(\cdot)$

Step 1: For each of the control inputs $u(\cdot)$ in $\mathcal{U}$, set the current state to the initial state and initialize a trajectory list with current states
Step 2: Compute the following state using the current set of states and control inputs
while $i \leftarrow t_1 : t_n$ **do**
  $\mathcal{X}_i = \mathcal{X}_{i-1} + \mathbf{f}(\mathcal{X}_{i-1})\Delta t$
end while
Step 3: Add the set of unique states to the trajectory list at its corresponding time steps
Step 4: Repeat steps 1 to 3 for different sets of control inputs $\mathcal{U}$
Step 5: The final trajectory list will consist of the over-approximated reachable set of dynamics for the given system

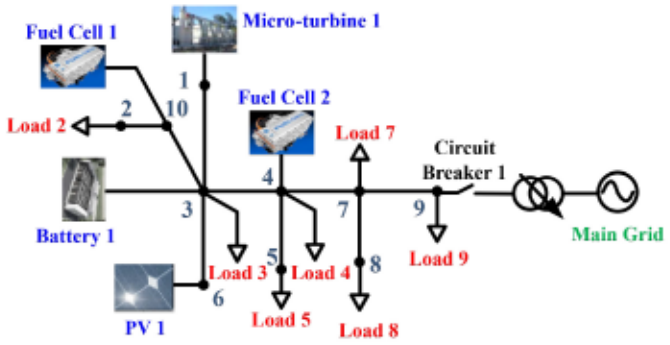

Fig. 3. 10 bus microgrid test system.

The projection of the reachable set to obtain the possible set of state variables is given by $\mathcal{R}^d([0, t_f])$ and the projection of the reachable set to obtain the possible set of algebraic variables is given by $\mathcal{R}^a([0, t_f])$.

The algorithm to compute the reachable set is given by Alg. 3.

Computation of reachable set is instrumental in designing controllers that guarantee certain performance or safety specifications for the different domain applications.

III. Numerical Examples

A 10 bus test system with multiple loads and DERs is developed to study the proposed hierarchical modularized SINDy-based adaptive droop controller cascaded with MPC. The one-line diagram of the system is shown in Fig. 3. The circuit breaker 1 is open and the microgrid operates in islanded mode. The loads based on the constant impedance model are connected at the buses 2,3,4,7,8 and 9. The DERs at buses 1 and 3 are regulated using a droop based controller. The other generational units are controlled using the standard PQ based controller. Transient dynamics are introduced in the islanded test system by varying the generations at different DERs and the loads connected to the different buses.

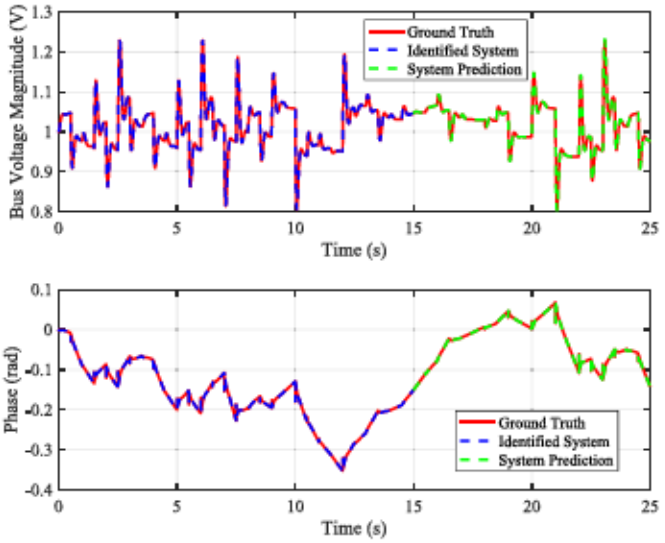

Fig. 4. Comparison of the identification and prediction model with the ground truth voltage at Bus 1.

A. Identification and Prediction Using the Proposed Algorithm

Input disturbances are introduced to the test system at very close time intervals to generate a dynamic data set for training the identification algorithm. The high fidelity model identified by the proposed hierarchical modularized physics informed sparse identification can be used to predict the future operations of the test system when new disturbances are applied.

Fig. 4 is used to display the effectiveness of the proposed algorithm in training and testing scenarios. The training data-set is used to train the algorithm which enables the identification model to learn the patterns and relationships between input variables and the state variables which can accurately explain the dynamics of the output variables. The algorithm's performance is then evaluated using the testing data-set which serves as an independent evidence to further elucidate the identification model's effectiveness.

It is rather easy to obtain the measurement of the bus voltage magnitude and phase angles using phasor measurement units. On the other hand, it is not common to obtain the time series measurement of the state variables. In this work, we assume the availability of all the state variables data to validate the proposed algorithm. This work also presumes the availability of the bus topology which can be used to determine the algebraic part of the set of DAEs which represents the overall microgrid test system.

The inverter d-axis modulation index of the droop-controlled DER is one of the most dominant state variables in a microgrid system and undergoes maximum dynamic variations. Fig. 5 shows zoomed in figures of the identification and prediction model of the state variable x_4, which represents the d-axis modulation index. The average root mean square error between the training and the identified data was found to be around $\pm 1.85e^{-5}\%$ across all the state variables. The average root mean square error between the testing data and the predicted data was also calculated and was found to be

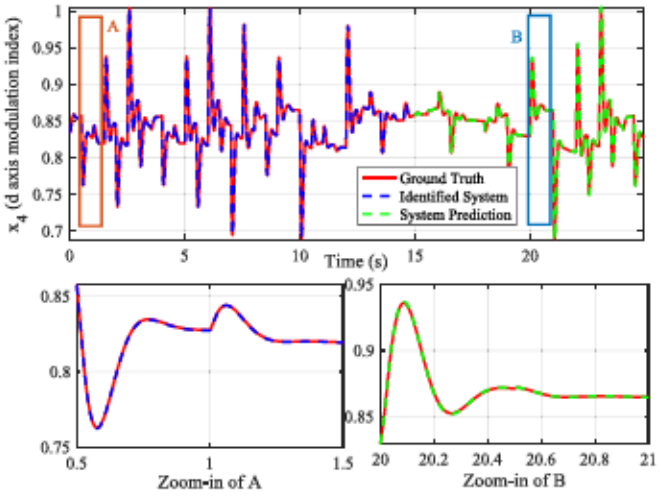

Fig. 5. Comparison of the identification and prediction model with the ground truth of the d-axis modulation index with zoomed in images.

around $\pm 6.46e^{-4}\%$ across all the state variables. This indicates that the algorithm has successfully learned the underlying patterns and is able to generalize its predictions to unseen data with good accuracy.

The modularized identification model was sampled at the rate of 1000 Hz (1000 samples per second) and recorded a computational time of 32.4*s* per module for identification. The centralized identification model required a sampling rate of 10000 Hz and required 672.07*s* for the overall computation. Thus, the modularized identification model is computationally more efficient and has lower reliance on data.

B. Improved Dynamic Performance With MPC for the Adaptive Droop Controller

The prediction model for the MPC is developed based on the hierarchical physics informed SINDy based identification. The *N*-steps after the current time step is predicted based on this algorithm to determine the future frequency deviations between the two droop controlled resources. A 3-step prediction horizon is utilized in this paper to minimize the error between the two droop controlled frequencies.

The positive impact in the reduction of system's transient dynamics due to the introduction of a model predictive controller in addition to the traditional droop-based double loop controller can be seen in Fig. 6. While the traditional droop controller with fixed droop coefficients can stabilize the microgrid system, it takes a longer response time to reach the steady state operation. The proposed MPC-based adaptive droop controller can quickly stabilize the frequency deviation between the different grid forming DERs.

The nominal frequency of the traditional droop controller oscillates between ± 0.25 Hz to provide the most optimal power sharing in the test system. The adaptive droop controller changes the droop coefficients at certain time intervals to minimize the overall deviations in the microgrid system and quickly restore the nominal frequency deviation to be between ± 0.02 Hz.

In Fig. 6, the performance with MPC is better in minimizing the frequency deviations between the two droop controlled

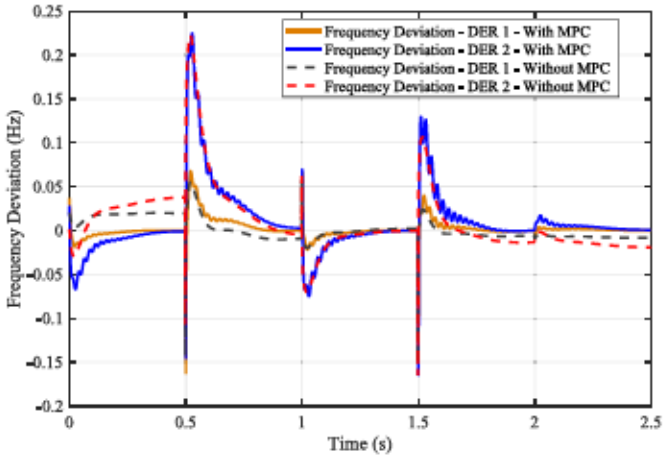

Fig. 6. Comparison of the frequency deviations in the system with and without MPC.

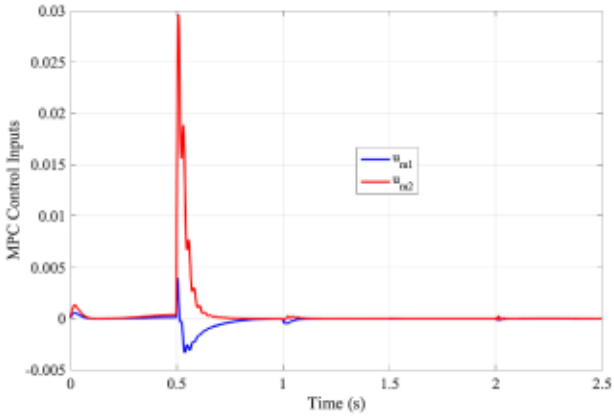

Fig. 7. Control inputs for the two adaptive droop controlled DERs.

DERs. The aim of the optimization problem is to reduce the frequency deviation between the two DERs to enable synchronization. Based on the plots, the DER controller with no MPC have not reached the synchronous state after 0.5s while the DERs with MPC have reached the synchronous state. Similar results can be clearly observed from the times 2s to 2.5s.

The control outputs generated by the MPC algorithm which is cascaded with the droop controller to generate the adaptive droop coefficient is plotted in Fig. 7. It can be seen that the control input values ranges from 0 to 0.1. Cascading this value with the traditional droop controller helps to achieve a smaller droop coefficient value. A smaller adapative droop coefficient has tighter load sharing, improved stability and better voltage regulations with smooth transitions between operations.

C. Reachable Set Computation

This test is performed to compute the reachable set under various active power and DC load fluctuations. As the set of reachable input disturbances changes in real time, the reachable set of the states and voltages results can be obtained to bound the overall system operations under extreme input variations. The bounds corresponding to the reachable set of voltage magnitude is shown in Fig. 8. It can be seen from

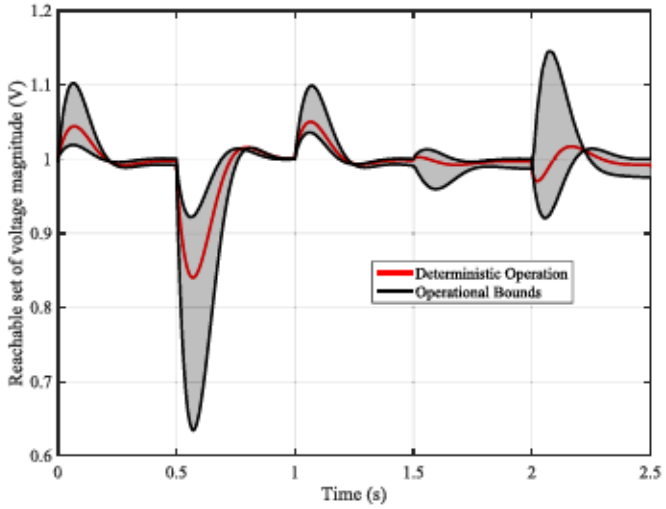

Fig. 8. Reachable set data of voltage magnitude at Bus 1.

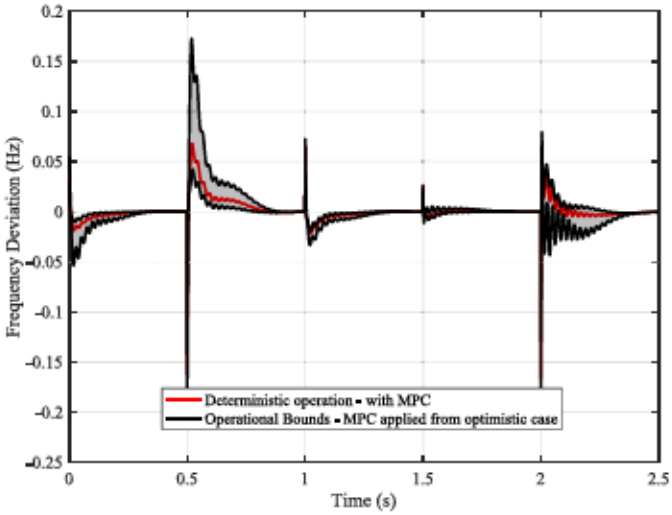

Fig. 9. Application of optimistic MPC inputs to the worst case reachable set.

the result that the deterministic operation of the system can be bounded by the worst case input disturbances in the active power and load changes.

D. Application of MPC Input to Stabilize Reachable Set of Operations

The computational complexity of MPC poses a great challenge by having a large computational time, especially when dealing with systems that require fast response times for online applications. Additionally, it is important to appropriately select the MPC tuning parameters, such as prediction horizon, control horizon, and constraints.

The reachable set typically represents the set of all possible worst case states that a given system can reach from the set of given initial conditions and input disturbances within a specified time horizon. In this work, the authors developed the control inputs required to stabilize the most optimistic case of deterministic operation in the microgrid system. The same set of control inputs were applied to stabilize the worst case scenario results generated by the reachable set computation.

Fig. 9 shows the results of the application of the result of the MPC developed for the optimistic case to the worst case operations of the microgrid bounds.

1) The worst case transient dynamics are stabilized by the control input generated for the best case scenario.
2) The new dynamics generated by the reachable set computation with MPC can bound the deterministic operation well.

The impact of the adaptive droop controller with MPC on the reachable set is illustrated by Fig. 10. The performance of the dynamics stabilization of the reachable set is better for the system with adaptive droop controller in comparison to the traditional droop controller. The reachable set is computed by varying the load demand and the DER power generations by ±80% to obtain the worst case microgrid operations.

E. Impact of Missing Data on System Identification

While the availability of all the state variables and output variables can help to identify the exact black-boxed system,

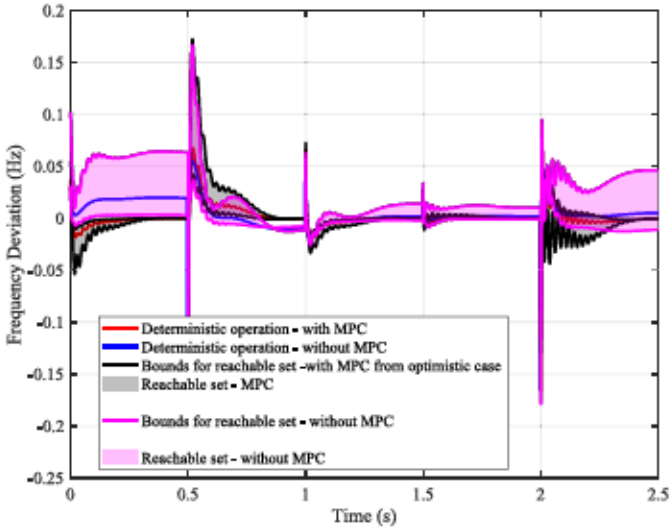

Fig. 10. Comparison of the reachable set data bounds with traditional droop controller and adaptive droop controller.

additional results corresponding to missing sensor data and its impact in the prediction model is provided in this section.

Fig. 11. and Fig. 12. represent the reduced accuracy in identification when the data corresponding to the PLL angle is missing. It can be observed that the impact of the missing PLL angle is more in the determination of q-axis modulation index than the determination of d-axis modulation index.

Fig. 13. has missing inverter modulation indices data. The d-axis modulation index data is represented by Ed and the q-axis modulation index data is represented by Eq. While the identification model is able to follow the dynamics of the true system, the amplitude is offset by Ed and Eq value due to the absence of these data. Thus, it can be verified that the PLL angle and modulation indices are the dominant states that determine the overall dynamics of the inverter based DER in a microgrid system.

While missing these critical data can be detrimental to the overall system identification, it has also been verified that

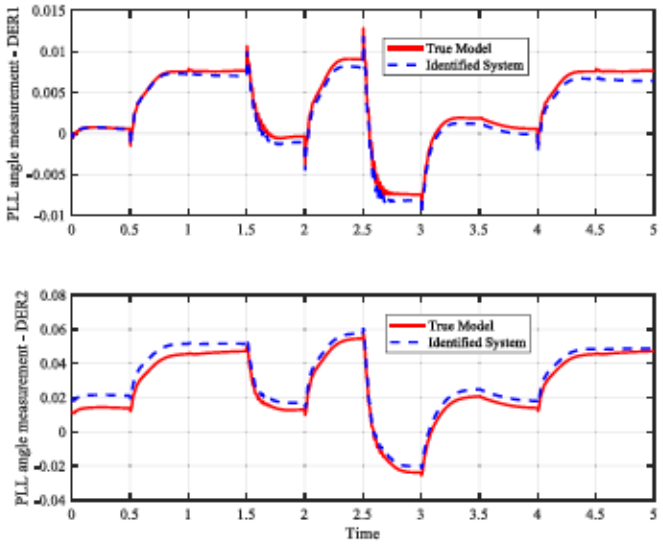

Fig. 11. System identification of DERs with missing PLL angle data.

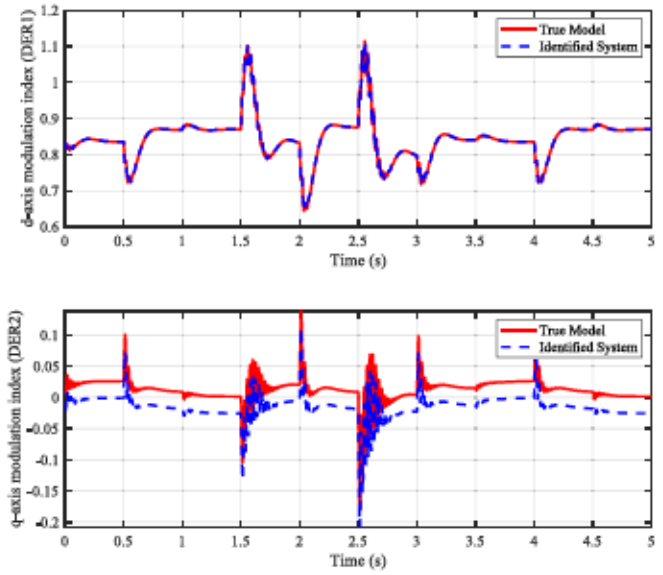

Fig. 12. System identification of modulation indexes with missing PLL angle data.

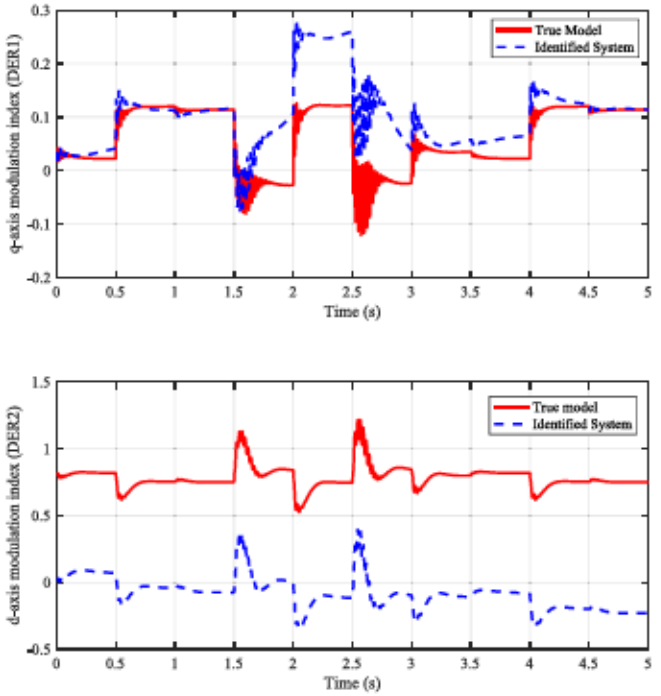

Fig. 13. System identification with missing modulation indices data.

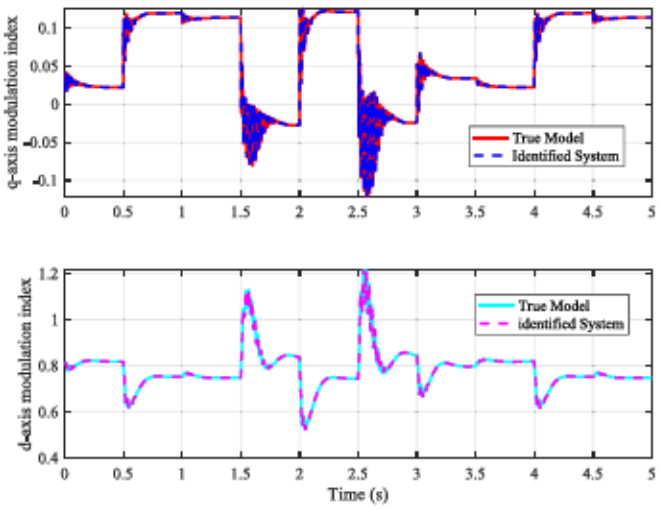

Fig. 14. System identification with missing data passed through the low pass filter.

the unavailability of certain state variables does not impact the identification model as much. Fig. 14. represents the case where the critical state variables' information is provided and other states in the controller are not being measured for system identification. While this model is not accurately representative of the original system, it does not inhibit the development of model predictive controller to optimize the system dynamics.

The collected data has also been processed to include 10% additional white gaussian noise (AWGN) to represent the potential issues caused by random noise while collecting data in real-time.

F. Investigation on Re-Configurable and Scalable Microgrid Dynamics

The modularization property of the proposed algorithms helps to individually integrate the identified DERs to a different system. Thus, the proposed model can be used for a large scale system, such as networked microgrid, in which computational efficiency would be a concern when developing the controller.

The reconfigured test system with 12 buses and an additional 6th DER (PV 2) is shown by Fig. 16. The simulation results of the system reconfiguration have been shown in Fig. 15., where the 5 DERs identified have been incorporated in a different test setup with 12 buses and additional variable loads. The results of the system scalability property are also explained in Fig. 15, where the identified Photo-Voltaic (PV) based inverter model is added as the 6th DER to the 12-bus test system. Based on the simulation results, we can observe successful prediction of this scaled and reconfigured test system. This is possible because of the block matrix

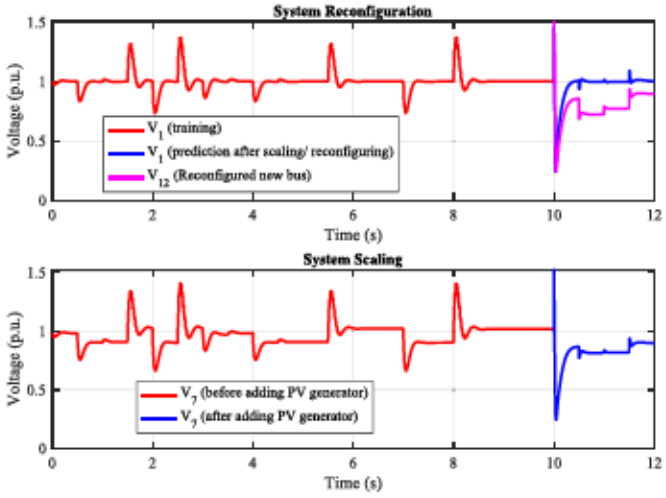

Fig. 15. (a) Representation of system reconfiguration from 10 bus system to 12 bus system (b) Representation of system scalability from 5 DER based system to 6 DER based system.

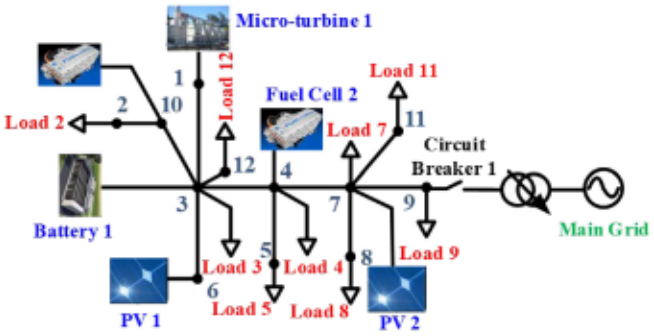

Fig. 16. 6-DER based 12 bus test system.

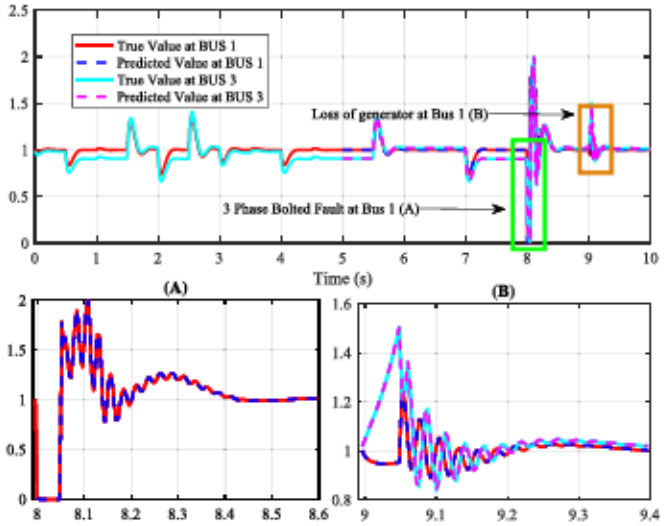

Fig. 17. Transient dynamics prediction under extreme grid events.

structure of the identified Ξ matrix and the modularization property of the proposed algorithm.

G. Response to Extreme Grid Events

The identified system has been tested under extreme grid events. The loss of generators, i.e., the micro-turbine outage is simulated by opening of inverter interconnection with the network from $t = 9$ s to $t = 9.1$ s. The testing data set includes a 3 phase LG (line to ground) fault for 0.05 s at Bus 1 and Bus 3 at $t = 8$ s. A close tracking of the microgrid transient dynamics by the identified model under extreme grid events can be observed in Fig. 17.

IV. Conclusion

This paper focuses on the development of an adaptive droop controller for frequency stabilization in microgrids. The adaptive droop controller is developed by cascading the traditional droop controller with a model predictive control algorithm that modifies the droop coefficients to achieve minimum frequency deviation. The availability of abundance of data in the power systems domain has been leveraged to develop a data-driven model that is employed in the MPC to predict the future behaviors of the system. A hierarchical modularized physics informed sparse identification method has been formulated to identify the system's transient dynamics. This method of identification is computationally efficient and has less reliance on high frequency data in comparison to the existing methods. The effectiveness of the proposed MPC is additionally tested by the application of the control inputs to the reachable set developed by the uncertainties in the system inputs. The reachable set dynamics are also quickly stabilized with minimal frequency deviations when the conventional droop controller is cascaded with the MPC. Numerical results have been discussed to explore the effectiveness of the overall algorithm in a microgrid system.

V. Future Work

There are multiple challenges in real time implementation of data-driven models to MPC. Efficient algorithms and hardware (e.g., GPUs) might be required to address and satisfy the high computational demand caused by the optimization problem that is solved by the MPC in real time. Incremental learning, parallel computing and simplified models can be used to balance accuracy and computational efficiency. Additionally, modular and scalable design approaches that allow easy adaptation and upgrades. The authors have recognized this key concern and as a step to port this knowledge of this paper to real world application, the RTDS real-time simulator can be utilized for a future work to validate the implementation of the proposed algorithm in real-time.

Appendix

Details regarding the microgrid test system and the control strategies used in this model are presented here. The system topology details for the 5-DER based 10-bus system are provided by Tables I, II, III.

The system has two specific control strategies corresponding to the grid-forming DERs (Droop Control) and grid-following DERs (P-Q control). The double-loop controller for the grid forming and grid following DERs is also shown in Fig. 18.

TABLE I
DER GENERATIONS AT EACH BUS

Bus	$P_n(kW)$	$Q_n(kVar)$
1	57.6	49.4
3	22.3	4.1
4	22.3	4.1
6	60.0	30.0
10	20.0	20.0

TABLE II
POWER LOADS AT EACH BUS

Bus	$P_n(kW)$	$Q_n(kVAR)$
2	12.75	7.91
3	17.75	5.91
4	17.75	5.91
5	42.51	26.34
7	61.15	20.63
8	40.00	37.90
9	12.75	7.91

TABLE III
LINE IMPEDANCE BETWEEN BUSES

From	To	R(Ω/km)	L(H/km)	Length(m)
10	2	0.0154	0.0468×10^{-3}	45
10	3	0.0021	0.0482×10^{-3}	30
3	1	0.0086	0.0408×10^{-3}	30
3	6	0.0096	0.1881×10^{-3}	50
3	4	0.0025	0.0964×10^{-3}	50
4	5	0.0033	0.0403×10^{-3}	50
4	7	0.0041	0.1446×10^{-3}	45
7	9	0.0346	0.0468×10^{-3}	20
7	8	0.0160	0.0890×10^{-3}	20

and Fig. 19. Equations explaining the details of the double-loop controller for the grid following and grid forming DERs are given below.

The differential equations ($\mathbf{f}(\mathbf{x}(t), \mathbf{y}(t), \mathbf{u}(t))$) that describe the dynamics of the control system for the grid-forming DER in Fig. 18 is given by (25)-(32). $\bar{V}_m$ and $\bar{\Delta\omega}$ references are defined by the droop controller parameters K_P and K_Q as

$$\bar{\Delta\omega} = \Delta\omega^* - K_P(P^* - P) \tag{23}$$
$$\bar{V}_m = V_m^* - K_Q(Q^* - Q) \tag{24}$$

The differential equations ($\mathbf{f}(\mathbf{x}(t), \mathbf{y}(t), \mathbf{u}(t))$) that describe the dynamics of the control system for the grid-following DER in Fig. 19 is given by (33)-(40). The algebraic equation, $\mathbf{g}(\mathbf{x}(t), \mathbf{y}(t), \mathbf{u}(t))$, describes the network power flow. The overall microgrid system can be described using the differential algebraic equations defined by $\mathbf{f}(\cdot)$ and $\mathbf{g}(\cdot)$.

$$\dot{x_1} = V_q - \bar{V}_q \tag{25}$$
$$\dot{x_2} = \Delta\omega \tag{26}$$
$$\dot{x_3} = \bar{V}_m - \sqrt{|V_d|^2 + |V_q|^2} \tag{27}$$
$$\dot{x_4} = \bar{\Delta\omega} - \Delta\omega \tag{28}$$
$$\dot{x_5} = \bar{I}_d - I_d \tag{29}$$
$$\dot{x_6} = \bar{I}_q - I_q \tag{30}$$
$$\dot{x_7} = \left(\bar{V}_d^{(\text{inv})} - x_7\right)/T_f \tag{31}$$
$$\dot{x_8} = \left(\bar{V}_q^{(\text{inv})} - x_8\right)/T_f \tag{32}$$
$$\dot{x_1} = V_q - \bar{V}_q \tag{33}$$

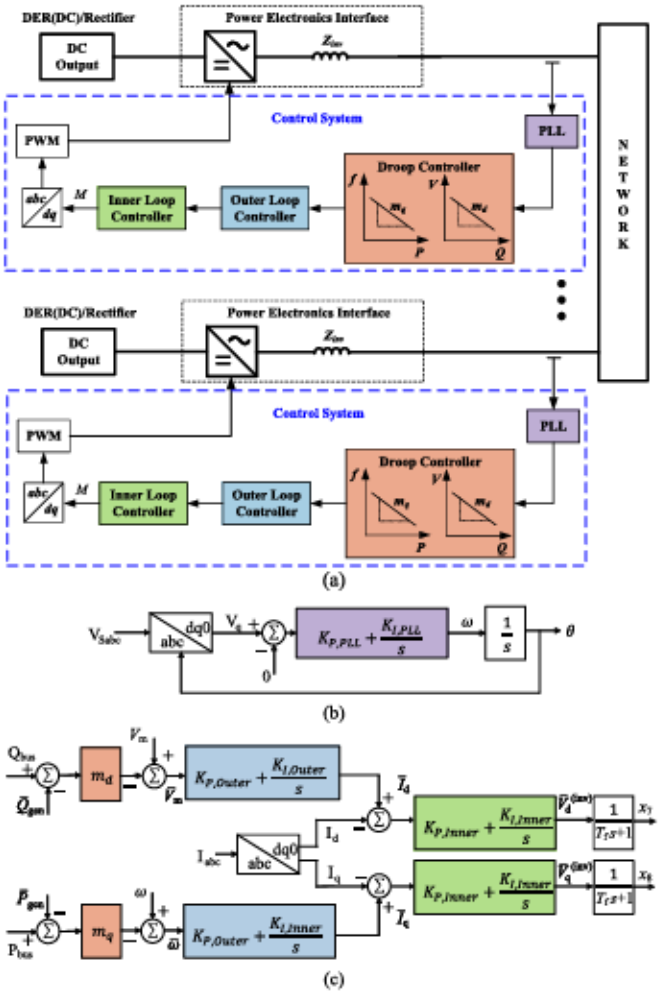

Fig. 18. Droop controller for grid forming DERs.

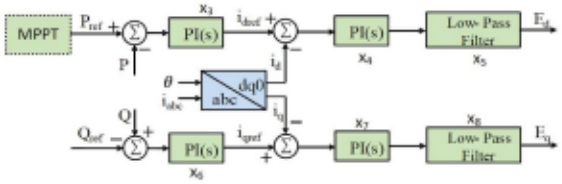

Fig. 19. Double loop controller for grid following DERs with/ without MPPT depending on the DER capability to dispatch active power.

$$\dot{x_2} = \Delta\omega \tag{34}$$
$$\dot{x_3} = P_{ref} - P \tag{35}$$
$$\dot{x_4} = Q_{ref} - Q \tag{36}$$
$$\dot{x_5} = \bar{I}_d - I_d \tag{37}$$
$$\dot{x_6} = \bar{I}_q - I_q \tag{38}$$
$$\dot{x_7} = \left(\bar{V}_d^{(\text{inv})} - x_7\right)/T_f \tag{39}$$
$$\dot{x_8} = \left(\bar{V}_q^{(\text{inv})} - x_8\right)/T_f \tag{40}$$

where, V_d and V_q represent the d-axis and q-axis bus voltages at the point of interconnection between the inverter and the network. $\Delta\omega$ is the change in frequency of the system calculated by the PLL design. T_f is the time constant used in the low pass filter.

TABLE IV
CONTINGENCIES FOR CREATING TRAINING DATASET

Time (s)	Pgen	Qgen	Load Variation
0.0	94% increase	84% increase	60% increase
0.5	6% increase	28% increase	50% increase
1.0	8% decrease	22% increase	20% increase
1.5	56% increase	2% increase	10% decrease
2.0	78% increase	18% decrease	5% increase
2.5	62% increase	16% increase	90% decrease
3.0	102% increase	18% increase	20% decrease
3.5	94% increase	18% decrease	60% increase
4.0	8% decrease	16% increase	50% increase
4.5	56% increase	18% increase	20% increase
5.0	78% increase	84% increase	10% decrease
5.5	62% increase	28% increase	5% increase
6.0	102% increase	22% increase	80% decrease
6.5	18% decrease	2% increase	5% decrease
7.0	36% increase	18% decrease	8% increase
7.5	28% increase	16% increase	18% decrease
8.0	46% increase	18% increase	28% increase
8.5	6% increase	98% increase	10% decrease
9.0	34% increase	2% decrease	20% decrease
9.5	14% increase	54% increase	28% decrease
10.0	6% increase	16% decrease	59% decrease
10.5	58% increase	58% increase	9% decrease
11.0	24% decrease	18% increase	5% increase
11.5	96% increase	16% decrease	5% increase
12.0	4% decrease	16% increase	21% increase
12.5	70% decrease	0% increase	0% increase
13.0	34% decrease	48% increase	90% decrease
13.5	66% increase	68% increase	150% increase
14.0	86% increase	30% increase	150% increase
14.5	4% decrease	34% decrease	71% increase

TABLE V
CONTINGENCIES FOR CREATING TESTING DATASET

Time(s)	Pgen	Qgen	Load Variation
15.0	52% increase	34% decrease	0% increase
15.5	70% decrease	80% decrease	90% decrease
16.0	34% decrease	0% increase	160% increase
16.5	34% decrease	40% increase	160% increase
17.0	42% increase	30% increase	88% increase
17.5	28% increase	34% decrease	27% increase
18.0	46% increase	34% decrease	10% decrease
18.5	46% increase	80% increase	10% decrease
19.0	34% increase	80% decrease	20% decrease
19.5	14% increase	8% decrease	22% decrease
20.0	12% decrease	54% increase	59% decrease
20.5	6% increase	16% decrease	2% increase
21.0	2% increase	58% increase	4% increase
21.5	78% increase	18% increase	90% decrease
22.0	62% increase	16% decrease	20% decrease
22.5	102% increase	16% decrease	60% increase
23.0	94% increase	48% decrease	50% increase
23.5	6% increase	18% decrease	20% increase
24.0	8% decrease	16% increase	10% decrease
24.5	2% increase	18% increase	5% increase

Multiple disturbances in the system load and power generation has been simulated to create transient dynamics in the microgrid model. A detailed description of the contingencies used is shown in Tables IV and V.

ACKNOWLEDGMENT

The authors would like to thank Dr. J. Nathan Kutz at the University of Washington for sharing the base code for SINDy. The authors would also like to thank Franck Djeumou for the preliminary discussions and knowledge sharing sessions. The authors would like to thank Siddharth Mahesh for his support which was instrumental for the timely completion of the work.

REFERENCES

[1] B. Lasseter, "Microgrids [distributed power generation]," in *Proc. IEEE Power Eng. Soc. Winter Meet. Conf.*, 2001, pp. 146–149.
[2] D. E. Olivares et al., "Trends in microgrid control," *IEEE Trans. Smart Grid*, vol. 5, no. 4, pp. 1905–1919, Jul. 2014.
[3] Y. Parag and M. Ainspan, "Sustainable microgrids: Economic, environmental and social costs and benefits of microgrid deployment," *Energy Sustain. Develop.*, vol. 52, pp. 72–81, Oct. 2019.
[4] C. Albea, C. Bordons, and M. A. Ridao, "Robust hybrid control for demand side management in islanded microgrids," *IEEE Trans. Smart Grid*, vol. 12, no. 6, pp. 4865–4875, Nov. 2021.
[5] P. Borazjani, N. I. A. Wahab, H. B. Hizam, and A. B. C. Soh, "A review on microgrid control techniques," in *Proc. IEEE Innovat. Smart Grid Technol. Asia (ISGT ASIA)*, 2014, pp. 749–753.
[6] M. Ramezani and S. Li, "Voltage and frequency control of islanded microgrid based on combined direct current vector control and droop control," in *Proc. IEEE Power Energy Soc. General Meet. (PESGM)*, 2016, pp. 1–5.
[7] M. Ramezani, S. Li, and Y. Sun, "Combining droop and direct current vector control for control of parallel inverters in microgrid," *Inst. Eng. Technol. Renew. Power Gener.*, vol. 11, pp. 107–114, Jan. 2017.
[8] L. Ahmethodzic and M. Music, "Comprehensive review of trends in microgrid control," *Renew. Energy Focus*, vol. 38, pp. 84–96, Sep. 2021. [Online]. Available: https://www.sciencedirect.com/science/article/pii/S1755008421000387
[9] A. Bani-Ahmed, M. Rashidi, A. Nasiri, and H. Hosseini, "Reliability analysis of a decentralized microgrid control architecture," *IEEE Trans. Smart Grid*, vol. 10, no. 4, pp. 3910–3918, Jul. 2019.
[10] M. H. Andishgar, E. Gholipour, and R. allah Hooshmand, "An overview of control approaches of inverter-based microgrids in islanding mode of operation," *Renew. Sustain. Energy Rev.*, vol. 80, pp. 1043–1060, Dec. 2017. [Online]. Available: https://www.sciencedirect.com/science/article/pii/S1364032117309140
[11] S. Sen and V. Kumar, "Microgrid control: A comprehensive survey," *Annu. Rev. Control*, vol. 45, pp. 118–151, Jun. 2018. [Online]. Available: https://www.sciencedirect.com/science/article/pii/S1367578818300373
[12] K. Rajesh, S. Dash, R. Rajagopal, and R. Sridhar, "A review on control of ac microgrid," *Renew. Sustain. Energy Rev.*, vol. 71, pp. 814–819, May 2017. [Online]. Available: https://www.sciencedirect.com/science/article/pii/S1364032116311613
[13] F. Alam, M. Ashfaq, S. S. Zaidi, and A. Y. Memon, "Robust droop control design for a hybrid AC/DC microgrid," in *Proc. UKACC 11th Int. Conf. Control (CONTROL)*, 2016, pp. 1–6.
[14] K. Liu, T. Liu, and D. J. Hill, "Decentralized MPC-based frequency control of networked microgrids," in *Proc. IEEE Innovative Smart Grid Technol. Asia (ISGT Asia)*, 2019, pp. 2704–2708.
[15] T. Liu, A. Chen, F. Gao, X. Liu, X. Li, and S. Hu, "Double-loop control strategy with cascaded model predictive control to improve frequency regulation for islanded microgrids," *IEEE Trans. Smart Grid*, vol. 13, no. 5, pp. 3954–3967, Sep. 2022.
[16] J. Wang et al., "An improved Koopman-MPC framework for data-driven modeling and control of soft actuators," *IEEE Robot. Autom. Lett.*, vol. 8, no. 2, pp. 616–623, Feb. 2023.
[17] J. Berberich, J. Köhler, M. A. Müller, and F. Allgöwer, "Data-driven model predictive control with stability and robustness guarantees," *IEEE Trans. Autom. Control*, vol. 66, no. 4, pp. 1702–1717, Apr. 2021.
[18] L. Hewing, K. P. Wabersich, M. Menner, and M. N. Zeilinger, "Learning-based model predictive control: Toward safe learning in control," *Annu. Rev. Control, Robot., Auton. Syst.*, vol. 3, pp. 269–296, May 2020.
[19] R. Kadali, B. Huang, and A. Rossiter, "A data driven subspace approach to predictive controller design," *Control Eng. Pract.*, vol. 11, no. 3, pp. 261–278, 2003.
[20] E. Kaiser, J. N. Kutz, and S. L. Brunton, "Sparse identification of nonlinear dynamics for model predictive control in the low-data limit," *Proc. Roy. Soc. A*, vol. 474, no. 2219, 2018, Art. no. 20180335.
[21] M. Raissi, P. Perdikaris, and G. E. Karniadakis, "Physics informed deep learning (Part-I): Data-driven solutions of nonlinear partial differential equations," 2017, *arXiv:1711.10561*.

[22] F. J. Montáns, F. Chinesta, R. Gómez-Bombarelli, and J. N. Kutz, "Data-driven modeling and learning in science and engineering," *Comptes Rendus Mécanique*, vol. 347, no. 11, pp. 845–855, 2019. [Online]. Available: https://www.sciencedirect.com/science/article/pii/S1631072119301809

[23] A. Nandakumar, Y. Li, and D. Huang, "Hierarchical multi-layered sparse identification for prediction of non-linear dynamics of reconfigurable microgrids," in *Proc. IEEE Int. Conf. Commun., Control, Comput. Technol. Smart Grids (SmartGridComm)*, 2023, pp. 1–6.

[24] Z. Chen, Y. Liu, and H. Sun, "Physics-informed learning of governing equations from scarce data," *Nat. Commun.*, vol. 12, p. 6136 , Oct. 2021.

[25] J. MacGregor and A. Cinar, "Monitoring, fault diagnosis, fault-tolerant control and optimization: Data driven methods," *Comput. Chem. Eng.*, vol. 47, pp. 111–120, Dec. 2012. [Online]. Available: https://www.sciencedirect.com/science/article/pii/S0098135412001937

[26] Y. S. Kim, "Comparison of the decision tree, artificial neural network, and linear regression methods based on the number and types of independent variables and sample size," *Expert Syst. Appl.*, vol. 34, no. 2, pp. 1227–1234, 2008. [Online]. Available: https://www.sciencedirect.com/science/article/pii/S0957417406004118

[27] T. Morstyn, B. Hredzak, R. P. Aguilera, and V. G. Agelidis, "Model predictive control for distributed microgrid battery energy storage systems," *IEEE Trans. Control Syst. Technol.*, vol. 26, no. 3, pp. 1107–1114, May 2018.

[28] M. Althoff, G. Frehse, and A. Girard, "Set propagation techniques for reachability analysis," *Annu. Rev. Control, Robot., Auton. Syst.*, vol. 4, no. 1, pp. 369–395, 2021. [Online]. Available: https://doi.org/10.1146/annurev-control-071420-081941

[29] Y. Li, Y. Zhang, D. Zhao, and L. Du, "Scalable distributed reachability analysis for cyber-physical networked microgrids with communication latency," in *Proc. IEEE Transp. Elect. Conf. Expo (ITEC)*, 2021, pp. 266–270.

[30] B. Schürmann, N. Kochdumper, and M. Althoff, "Reachset model predictive control for disturbed nonlinear systems," in *Proc. IEEE Conf. Decis. Control (CDC)*, 2018, pp. 3463–3470.

[31] T. J. Bird, N. Jain, H. C. Pangborn, and J. P. Koeln, "Set-based reachability and the explicit solution of linear MPC using hybrid Zonotopes," in *Proc. Am. Control Conf. (ACC)*, 2022, pp. 158–165.

[32] F. Djeumou, A. Zutshi, and U. Topcu, "On-the-fly, data-driven reachability analysis and control of unknown systems: An F-16 aircraft case study," in *Proc. 24th Int. Conf. Hybrid Syst., Comput. Control*, 2021, pp. 1–2.

[33] X. Xu, H. Jia, H.-D. Chiang, D. C. Yu, and D. Wang, "Dynamic modeling and interaction of hybrid natural gas and electricity supply system in microgrid," *IEEE Trans. Power Syst.*, vol. 30, no. 3, pp. 1212–1221, May 2015.

[34] Y. Li and P. Zhang, "Reachable set calculation and analysis of microgrids with power-electronic-interfaced renewables and loads," in *Proc. IEEE Power Energy Soc. General Meet. (PESGM)*, 2018, pp. 1–5.

[35] S. L. Brunton, J. L. Proctor, and J. N. Kutz, "Discovering governing equations from data by sparse identification of nonlinear dynamical systems," *Proc. Nat. Acad. Sci.*, vol. 113, no. 15, pp. 3932–3937, 2016.

[36] U. Fasel, E. Kaiser, J. N. Kutz, B. W. Brunton, and S. L. Brunton, "SINDy with control: A tutorial," in *Proc. 60th IEEE Conf. Decis. Control (CDC)*, 2021, pp. 16–21.

[37] A. Nandakumar, Y. Li, D. Zhao, Y. Zhang, and T. Hong, "Sparse identification-enabled data-driven modeling for nonlinear dynamics of microgrids," in *Proc. IEEE Power Energy Soc. Gener. Meet. (PESGM)*, 2022, pp. 1–5.

[38] A. Nandakumar et al., "Data-driven modeling of microgrid transient dynamics through Modularized sparse identification," *IEEE Trans. Sustain. Energy*, vol. 15, no. 1, pp. 109–122, Jan. 2024.

[39] S. Ahmad, S. Mekhilef, and H. Mokhlis, "DQ-axis synchronous reference frame based PQ control of grid connected AC microgrid," in *Proc. IEEE Int. Conf. Comput., Power Commun. Technol. (GUCON)*, 2020, pp. 842–847.

[40] U. B. Tayab, M. A. B. Roslan, L. J. Hwai, and M. Kashif, "A review of droop control techniques for microgrid," *Renew. Sustain. Energy Rev.*, vol. 76, pp. 717–727, Sep. 2017.

[41] A. Tuladhar, H. Jin, T. Unger, and K. Mauch, "Parallel operation of single phase inverter modules with no control interconnections," in *Proc. APEC 97-Appl. Power Electron. Conf.*, 1997, pp. 94–100.

[42] E. F. Camacho and C. B. Alba, *Model Predictive Control*. London, U.K.: Springer, 2013.

[43] Y. Li and N. R. Chaudhuri, "Resilience analysis of islanded microgrids with droop control through reachable set computation," in *Proc. IEEE Power Energy Soc. Gener. Meet. (PESGM)*, 2022, pp. 1–5.

[44] F. Djeumou, A. P. Vinod, E. Goubault, S. Putot, and U. Topcu, "On-the-fly control of unknown systems: From side information to performance guarantees through reachability," *IEEE Trans. Autom. Control*, vol. 68, no. 8, pp. 4857–4872, Aug. 2023.

[45] M. Althoff and B. H. Krogh, "Reachability analysis of nonlinear differential-algebraic systems," *IEEE Trans. Autom. Control*, vol. 59, no. 2, pp. 371–383, Feb. 2014.

[46] "2. Theory of DAE's," in *Numerical Solution of Initial-Value Problems in Differential-Algebraic Equations*. Philadelphia, PA, USA: Soc. Ind. Appl. Math., pp. 15–39. [Online]. Available: https://epubs.siam.org/doi/abs/10.1137/1.9781611971224.ch2

Apoorva Nandakumar received the B.Tech. degree from the Department of Instrumentation and Control Engineering, National Institute of Technology, Tiruchirappalli, India, in 2019, and the M.S. and Ph.D. degrees with specific focus on power electronics and data-driven applications of power systems from the Department of Electrical Engineering, The Pennsylvania State University in 2021 and 2024, respectively. Her research interests includes data driven modeling, stability analysis and control of networked microgrids, and software defined networking.

Yan Li (Senior Member, IEEE) received the Ph.D. degree in electrical engineering from the University of Connecticut, Storrs, CT, USA, in 2019, and the Ph.D. degree in electrical engineering from Tianjin University, Tianjin, China, in 2013. She is currently an Assistant Professor with the School of Electrical Engineering and Computer Science, The Pennsylvania State University, University Park, PA, USA. Her research interests include cyber-physical microgrids, quantum computing, data-driven modeling and control, stability and resilience analysis, cybersecurity, reachability, and software-defined networking.

Zhe Xu (Member, IEEE) received the B.S. and M.S. degrees in electrical engineering from Tianjin University, Tianjin, China, in 2011 and 2014, respectively, and the Ph.D. degree in electrical engineering from Rensselaer Polytechnic Institute, Troy, NY, USA, in 2018. He is currently an Assistant Professor with the School for Engineering of Matter, Transport, and Energy, Arizona State University (ASU), Tempe, AZ, USA. Before joining ASU, he was a Postdoctoral Researcher with the Oden Institute for Computational Engineering and Sciences, The University of Texas at Austin, Austin, TX, USA. His research interests include formal methods, autonomous systems, control systems, and reinforcement learning. He is a recipient of the Howard Kaufman '62 Memorial Fellowship', the ASU Fulton Schools of Engineering Top 5 % Teaching Recognition Award, and the NSF CAREER Award.

Daning Huang (Member, IEEE) received the Ph.D. degree in aerospace engineering from the University of Michigan, Ann Arbor, in 2019. He is currently an Assistant Professor in aerospace engineering with The Pennsylvania State University. His research interests include data-driven modeling, analysis, and control and optimization of multi-disciplinary dynamical systems.